The Journal of Experimental Biology 212, 1731-1744
Published by The Company of Biologists 2009
doi:10.1242/jeb.029306

Review

Epithelial ultrastructure and cellular mechanisms of acid and base transport in the *Drosophila* midgut

Shubha Shanbhag and Subrata Tripathi*
Tata Institute of Fundamental Research, Colaba, Mumbai 400 005, India
*Author for correspondence (e-mail: tripathi@tifr.res.in)

Accepted 16 March 2009

Summary

There is a resurgence of interest in the *Drosophila* midgut on account of its potential value in understanding the structure, development and function of digestive organs and related epithelia. The recent identification of regenerative or stem cells in the adult gut of *Drosophila* has opened up new avenues for understanding development and turnover of cells in insect and mammalian gastrointestinal tracts. Conversely, the physiology of the *Drosophila* gut is less well understood as it is a difficult epithelial preparation to study under controlled conditions. Recent progress in microperfusion of individual segments of the *Drosophila* midgut, in both larval and adult forms, has enabled ultrastructural and electrophysiological study and preliminary characterization of cellular transport processes in the epithelium. As larvae are more active feeders, the transport rates are higher than in adults. The larval midgut has at least three segments: an anterior neutral zone, a short and narrow acid-secreting middle segment and a long and wider posterior segment (which is the best studied) that secretes base (probably HCO_3^-) into the lumen. The posterior midgut has a lumen-negative transepithelial potential (35–45 mV) and a high resistance (800–1400 Ω.cm^2) that correlates with little or no lateral intercellular volume. The primary transport system driving base secretion into the lumen appears to be a bafilomycin-A_1-sensitive, electrogenic H^+ V-ATPase located on the basal membrane, which extrudes acid into the haemolymph, as inferred from the extracellular pH gradients detected adjacent to the basal membrane. The adult midgut is also segmented (as inferred from longitudinal gradients of pH dye-indicators in the lumen) into anterior, middle and posterior regions. The anterior segment is probably absorptive. The middle midgut secretes acid (pH<4.0), a process dependent on a carbonic-anhydrase-catalysed H^+ pool. Cells of the middle segment are alternately absorptive (apically amplified by ≈9-fold, basally amplified by >90-fold) and secretory (apically amplified by >90-fold and basally by ≈10-fold). Posterior segment cells have an extensively dilated basal extracellular labyrinth, with a volume larger than that of anterior segment cells, indicating more fluid reabsorption in the posterior segment. The luminal pH of anterior and posterior adult midgut is 7–9. These findings in the larval and adult midgut open up the possibility of determining the role of plasma membrane transporters and channels involved in driving not only H^+ fluxes but also secondary fluxes of other solutes and water in *Drosophila*.

Key words: stereology, microperfusion, H^+ V-ATPase, carbonic anhydrase, ion-selective microelectrodes, SIET, H^+ gradients, surface pH.

Introduction

The insect gut carries out some of the most vital functions of nutrition and solute and water balance of the organism. It is the first line of defence against ingested pathogens and also the portal of entry of viruses and parasites for which insect species are major vectors. The gut epithelium, with its luminal contents, has a fascinating dynamic structure and nutrient circulation pattern, the importance of which is not completely understood. The diet of insects is of such wide variety in terms of texture, composition, fluidity and mechanical properties, from liquid plant sap to solid bark, from whole blood to decomposing insects, that the digestive system of each insect, in larval or adult form, male or female, appears specialized in overall structure and in biochemical machinery to handle its staple ingested material. The uptake of solutes and water by the gut is also vital for the maintenance of the composition, pH and osmolarity of the haemolymph within a permissible range. However, the integrated role of segments of the gut (midgut and hindgut) and the Malpighian tubules in overall fluid and electrolyte balance is far from clear in most insects. Whereas fluid secretion and excretion of normal nitrogenous metabolic end-products, toxins, pesticides, etc. by Malpighian tubules have been studied extensively (Beyenbach, 2001; Dow et al., 1997; Dow and Davies, 2001; Maddrell and O'Donnell, 1992; O'Donnell and Spring, 2000), the midgut and hindgut of most species have not been as amenable to study, possibly on account of their musculature.

Insect organs such as the midgut are appealing as the epithelium is single-layered and the number and type of cells are limited. This permits *in vitro* physiological studies with excellent control of key variables: (1) solution composition at the apical or basal surfaces with minimum diffusion barriers, (2) hydrostatic pressure, particularly across the intercellular septa or tight-junctions, and (3) electrical potential (Tripathi and Boulpaep, 1989). Furthermore, the cells should be accessible with conventional and ion-selective microelectrodes, which permit evaluation of the cellular handling of ingested primary electrolytes such as K^+, Na^+, H^+, Cl^-, HCO_3^-, and possible organic substrates co-transported with these ions, and also patch-clamp and fluorescence studies of the cytosol. Combined with other studies such as imaging of transparent gut structures with pH-indicator dyes, localization of membrane transport proteins with fluorescent-labelled antibodies, and scanning of extracellular fluid adjacent to individual cells for ion gradients (the SIET

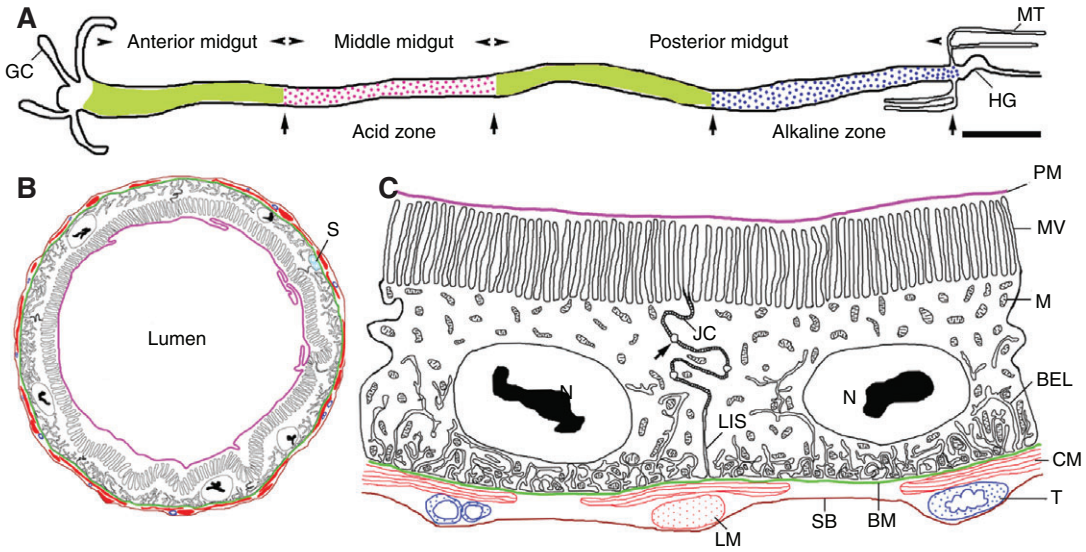

Fig. 1. (A) Drawing of larval midgut of *Drosophila melanogaster* showing various segments and the intraluminal pH zones. The luminal content of the anterior segment and the anterior part of the posterior segment is between neutral to mild alkalinity (pH>7 and <8; green), the middle segment is highly acidic (pH<3.0; magenta dots) and the posterior part of the posterior segment is highly alkaline (pH>10; blue dots). GC, gastric caeca; HG, hindgut; MT, Malpighian tubules. (B) Schematic representation of a cross-section of the posterior region of the larval posterior midgut showing the arrangement of peritrophic membrane (magenta), epithelial cells (black), basement membrane (green), muscle fibres (red), regenerative cells or stem cells (light blue, marked S) and serosal barrier (brown). (C) General organization of two adjacent epithelial cells, lateral dimensions compressed. Colour coding is the same as in B. The arrow denotes very small lateral intercellular spaces. BEL, basal extracellular labyrinth; BM, basement membrane; CM, circular muscle; JC, junctional complex; LIS, lateral intracellular septum; LM, longitudinal muscle; M, mitochondria; MV, microvilli; N, nucleus; PM, peritrophic membrane; SB, serosal barrier; T, tracheole.

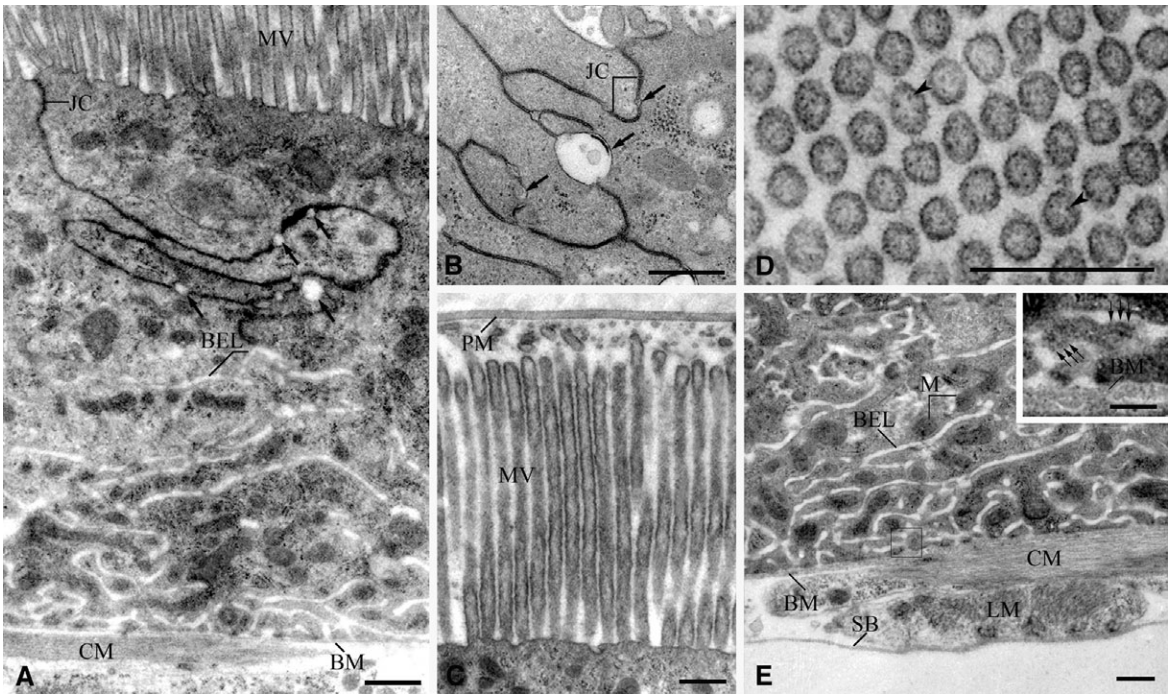

Fig. 2. Unperfused larval posterior midgut. (A) Section through two adjacent enterocytes of unperfused posterior midgut of larva depicting the intercellular septum from the junctional complex (JC) to the basal extracellular labyrinth (BEL). The lateral intracellular space is absent except for a few small dilations (arrows). The apical region of these cells contains microvilli (MV), and the basal region rests on the basement membrane (BM). An inner layer of circular muscles (CM) is also seen; magnification ×13,200; scale bar, 1 μm. (B) Magnified view of an apical region with intercellular septal JC and dilations (arrows); magnification ×37,300; scale bar, 0.5 μm. (C) Apical region of epithelial cell showing MV separated from the gut lumen by a single peritrophic membrane (PM); magnification ×21,000; scale bar, 0.5 μm. (D) Cross-section of MV showing outer surfaces with fine fuzzy material and cytoplasmic surfaces containing portasome-like particles (arrowheads); magnification ×84,000; scale bar, 0.5 μm. (E) Section through a basal region of an epithelial cell showing an extensive BEL closely associated with mitochondria (M). The basement membrane (BM) is separated from the haemolymph by inner CM, outer longitudinal muscle (LM) and the outermost thin serosal barrier (SB); magnification ×16,700; scale bar, 0.5 μm. The BEL is lined by particles of <20 nm diameter (small arrows, in inset). The inset is a magnified view of the boxed region in E; magnification ×54,000; inset scale bar, 0.25 μm.

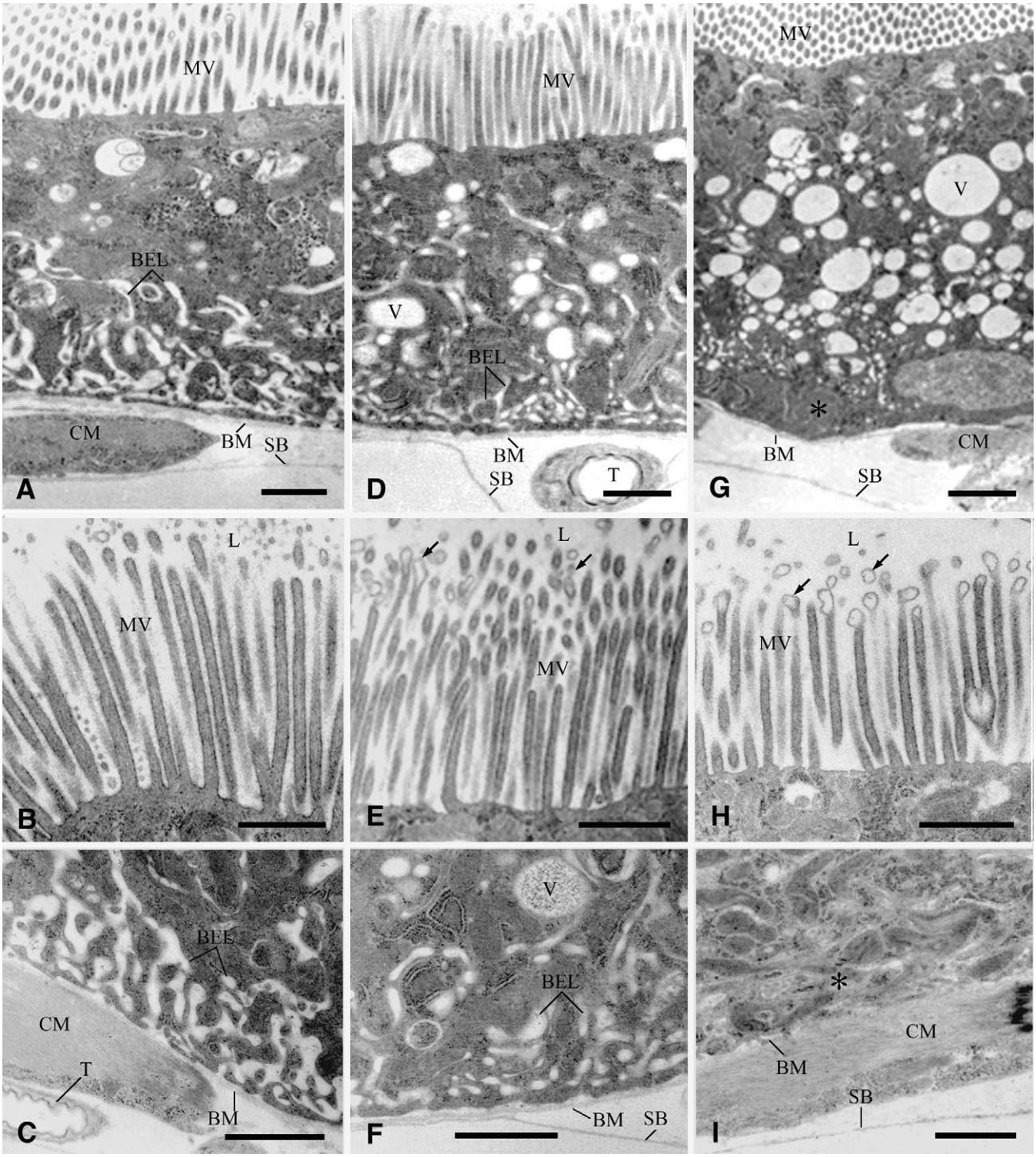

Fig. 3. Perfused larval posterior midgut. (A–C) Sections of larval posterior midgut epithelial cell perfused with bilateral Hepes Ringer solution. (A) Microvillar brush border (MV) and extensive basal extracellular labyrinth (BEL); magnification ×11,700. (B) Removal of the peritrophic membrane ensures direct access of intact microvilli (MV) to the luminal (L) perfusion solution. magnification ×16,000. (C) Basal region of the cell shows basement membrane (BM), enclosing a significant BEL; magnification ×17,400. (D–F) Sections of larval posterior midgut epithelial cell perfused with Hepes Ringer in the bath and Na^+-free Hepes Ringer in the lumen. (D) The MV are intact, but BEL volume is reduced and several large intracellular vacuoles (V) are found in the cytoplasm; magnification ×12,000. (E) MV have many vesicles budding off from them (arrows); magnification ×16,700. (F) Magnified view of the basal region of the cell with reduced BEL volume; magnification ×18,700. (G–I) Perfusion with bilateral Na^+-free Hepes Ringer. (G) The cell is filled with a large number of intracellular vacuoles (V); magnification ×11,700. (H) MV height is reduced, and there are several dilated vesicles (arrows) budding off from MV tips; magnification ×16,700. (I) Basal region of the cell is devoid of basal extracellular labyrinth (asterisk); magnification ×14,000. CM, circular muscle; SB, serosal barrier; T, tracheole. Scale bars (A–I), 1.0 μm.

Table 1. Quantitative ultrastructural analysis of larval posterior midgut segment in *Drosophila melanogaster*

	Unperfused	Perfused, single-end cannulated			
Luminal solution:	HCO_3^--R	Hepes-R	Na^+-free-R	Hepes-R	Na^+-free-R
Bath solution:	HCO_3^--R	Hepes-R	Hepes-R	Na^+-free-R	Na^+-free-R
Apical membrane gain by folding (per cell)	1.44	1.15	1.06	1.25	0.82
Mean microvillar amplification	44.76	34.22	38.75	29.37	15.56
Mean luminal membrane surface (excluding microvilli) (10^3 μm^2 mm^{-1} length)	506.0	471.43	471.43	471.43	471.43
Mean apical membrane area (10^6 μm^2 mm^{-1} length)	22.65	16.13	18.27	13.85	7.34
Mean basement membrane surface area (10^3 μm^2 mm^{-1} length)	597.14	534.29	534.29	534.29	534.29
Basal extracellular labyrinth amplification*	11.2±1.2	13.2±0.5	8.39±0.6	2.13±0.43	1.77±0.93
Mean cell volume (10^6 μm^3 mm^{-1} length)	5.64	3.71	3.84	3.98	2.96
Mean basal extracellular labyrinth volume (10^6 μm^3 mm^{-1} length)	0.59 (10.5%)	0.43 (11.6%)	0.26 (6.8%)	0.05 (1.3%)	0.024 (0.8%)
Mean basal membrane area (10^6 μm^2 mm^{-1} length)	6.69	7.05	4.48	1.14	0.95
Ratio of microvillar amplification/BEL amplification	3.99	2.59	4.62	13.79	8.79
Vacuolar volume* (10^6 μm^3 mm^{-1} length)	0.04±0.01	0.07±0.01	0.28±0.07	0.37±0.06	0.34±0.12

Solutions present prior to fixation are shown in parentheses. Data are reported as means from at least 10 cells or at least 10 complete tubular midgut wall sections. *Data are means ± s.e.m. Fixation protocol and morphometric methods have been described in detail previously (Shanbhag and Tripathi, 2005).

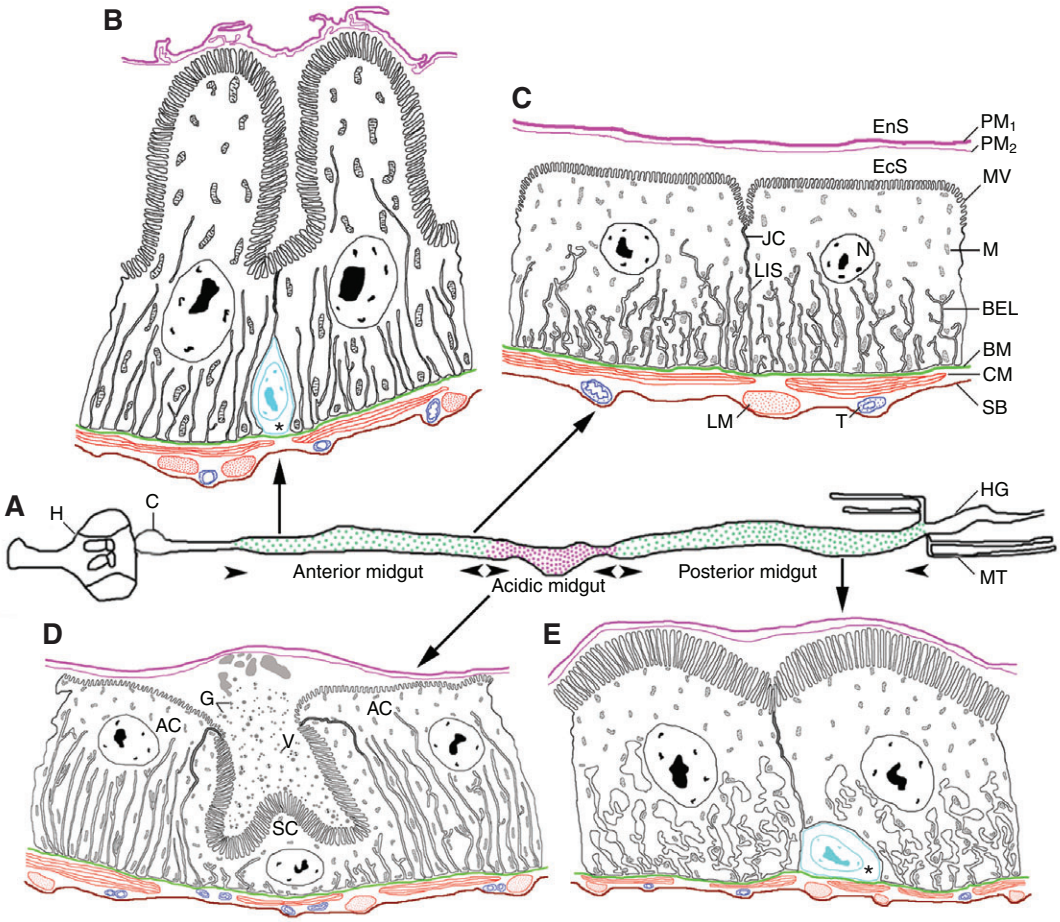

Fig. 4. (A) Line diagram of adult gut showing the intraluminal pH in various midgut regions. The luminal contents of anterior and posterior midgut segments are mildly alkaline (pH 7–9; green dots), while the middle midgut segment is acidic (pH<4.0; magenta dots). C, cardia; H, head; HG, hindgut; MT, Malpighian tubules. (B–E) General organization of adjacent epithelial cells of various segments of adult midgut showing the arrangement of peritrophic membrane (magenta), epithelial cells (black), basement membrane (green), muscle fibres (red), regenerative cells or stem cells (light blue, marked *) and serosal barrier (brown). (B,C) Anterior and posterior region of the anterior midgut, respectively. (D) Acidic middle midgut. The apical region of the secretory cell (SC) extrudes a large number of electron-lucent vesicles (V) and vesicles containing electron-dense granules (G). (E) Posterior midgut. AC, absorptive cell; BEL, basal extracellular labyrinth; BM, basement membrane; CM, circular muscle; EcS, ectoperitrophic space; EnS, endoperitrophic space; G, granules; JC, junctional complex; LIS, lateral intracellular septum; LM, longitudinal muscle; M, mitochondria; MV, microvilli; N, nucleus; PM_1 and PM_2, peritrophic membranes; SB, serosal barrier; T, tracheole.

Table 2. Quantitative ultrastructural analysis of bilaterally perfused anterior and posterior midgut segments in adult *Drosophila melanogaster*

	Anterior segment		Posterior segment	
	Unperfused	Perfused	Unperfused	Perfused
Apical membrane gain by folding (per cell)	~2	~1.73	~1.6	~2.37
Mean microvillar amplification*	142.9±7.4 (*N*=8)	35.1±2.3 (*N*=15)	98.1±4.5 (*N*=6)	64.9±5.2 (*N*=17)
Mean luminal membrane surface (excluding microvilli) (10^3 μm^2 mm^{-1} length)	661.3	766.4	590.9	880.0
Mean apical membrane area (10^6 μm^2 mm^{-1} length)	94.5	26.9	58.0	57.1
Mean basement membrane surface area (10^3 μm^2 mm^{-1} length)	440.0	422.5	502.9	468.9
Basal extracellular labyrinth amplification*	43.4±2.7 (*N*=11)	26.0±1.3 (*N*=21)	25.7±2.1 (*N*=14)	25.9±3.4 (*N*=6)
Mean cell volume (10^6 μm^3 mm^{-1} length)	6.5	7.7	5.5	6.2
Mean basal extracellular labyrinth volume (10^6 μm^3 mm^{-1} length)	0.65 (10%)	1.2 (15.1%)	1.25 (22.9%)	1.0 (15.7%)
Mean basal membrane area (10^6 μm^2 mm^{-1} length)	19.1	11.0	12.9	12.2
Ratio of microvillar amplification/BEL amplification	3.29	1.35	3.82	2.51

*Data are means ± s.e.m.

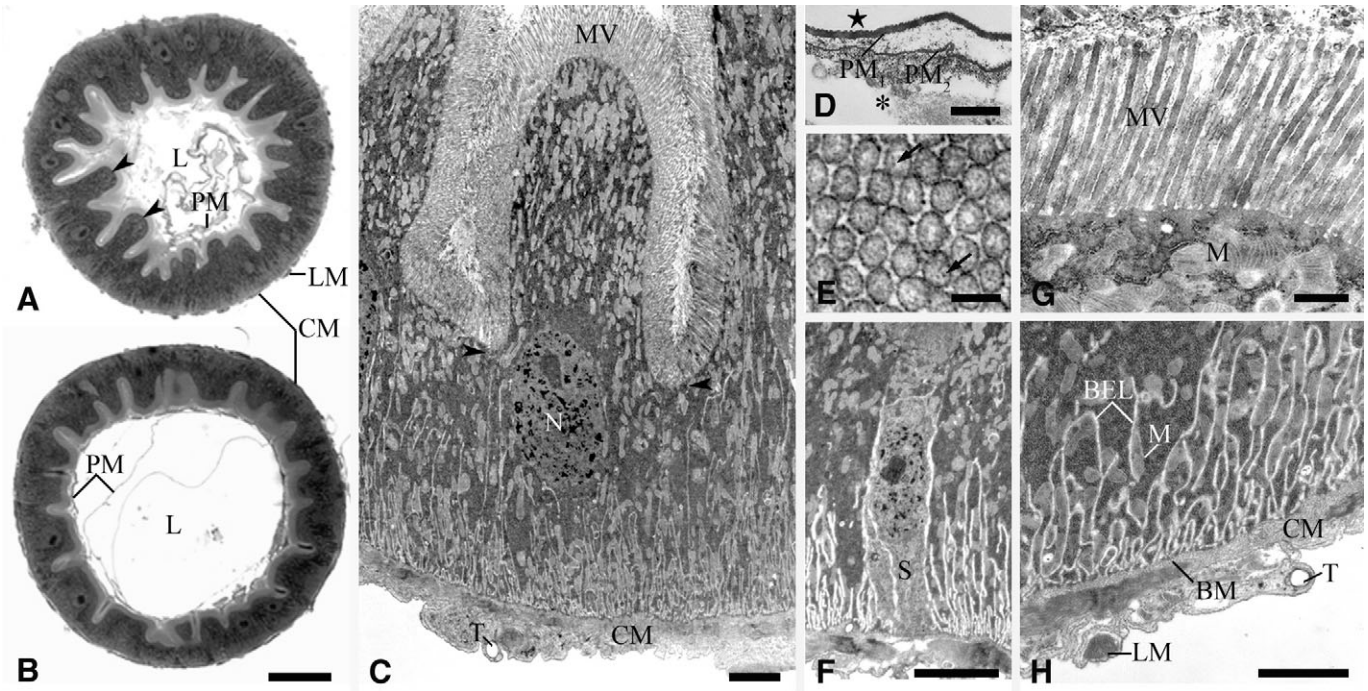

Fig. 5. Unperfused adult anterior midgut. (A,B) Light micrographs of cross-sections of anterior and posterior regions, respectively, of an adult anterior midgut. Epithelial cells show large spherical or oval nuclei at the centre. (A) Enterocytes of the anterior region are taller, with a central cytoplasmic dome into the lumen (arrowheads); magnification ×400. (B) Posterior cells are large, cuboidal cells; magnification ×400. Scale bars (A,B), 25 μm. (C) A single epithelial cell sectioned through the anterior region of the anterior adult midgut has a large oval-shaped nucleus (N) and a central cytoplasmic dome. The apical region of the cell contains a well-developed microvillar (MV) brush-border. Arrowheads denote the region from where the intracellular junctional complexes begin; magnification ×4400; scale bar, 2 μm. (D) Section through double-layered peritrophic membranes (PM), an inner thick one (PM_1) that surrounds the food, and an outer thin one (PM_2) that bounds the ectoperitrophic space (asterisk) with the MV; star, ectoperitrophic space; magnification ×18,700; scale bar, 0.5 μm. (E) Cross-sections of MV showing small portasome-like particles on their cytoplasmic side (arrows); magnification ×100,000; scale bar, 0.1 μm. (F) An elongated regenerative or stem cell (S) located between the two enterocytes; magnification ×8100; scale bar, 2.0 μm. (G) Longitudinal section through a portion of brush-border with MV; the apical region of the cell has several large mitochondria (M); magnification ×20,100; scale bar, 0.5 μm. (H) Section through a basal region of an enterocyte showing infoldings of the basal extracellular labyrinth (BEL). The basement membrane (BM) is separated from the haemolymph by inner circular muscle (CM) and outer longitudinal muscle (LM). T, tracheole; magnification ×8800; scale bar, 0.5 μm.

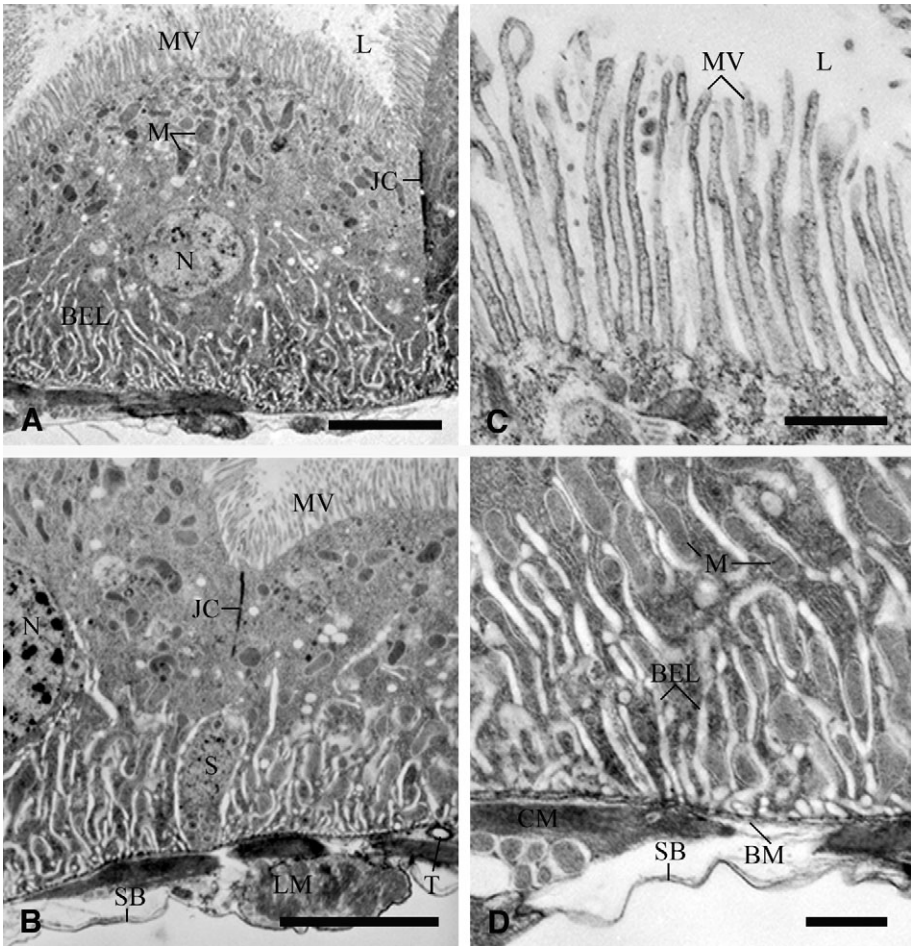

Fig. 6. Perfused adult anterior midgut. (A) Epithelium showing centrally located nucleus (N) and many apically located mitochondria (M). The basal extracellular labyrinth (BEL) extends up to almost half the cell height. L, lumen; MV, microvilli; JC, junctional complex; magnification ×2700; scale bar, 5.0 μm. (B) Section through two adjacent epithelial cells of a perfused adult anterior midgut shows a basal regenerative cell (S) between them; magnification ×3780; scale bar, 5.0 μm. (C) Apical region of the epithelial cell of perfused adult anterior midgut cells showing MV that are in direct access to the luminal solution; magnification ×12,000; scale bar, 1.0 μm. (D) Basal region has many mitochondria (M). BM, basement membrane; CM, circular muscle; LM, longitudinal muscle; SB, serosal barrier; T, tracheole; ×10,000; scale bar, 1.0 μm.

technique), it is possible to get valuable information on the functional organization of the gut, its developmental changes and its ultrastructural design (Boudko et al., 2001a; Onken et al., 2006).

The midgut of several insect species with a wide variety of diet has been studied at a cellular level (Anderson and Harvey, 1966; Cioffi, 1979; Clements, 1992; Dow, 1984; Dow, 1986; Dow and Peacock, 1989; Lehane and Billingsley, 1996; Moffett and Cummings, 1994; Okech et al., 2008; Onken et al., 2008; Patrick et al., 2006; Smith et al., 2007; Smith et al., 2008; Volkmann and Peters, 1989a; Volkmann and Peters, 1989b; Zhuang et al., 1999). These studies have revealed large longitudinal gradients of pH along the length of the gut. However, the cellular basis of generation of these gradients and their biological significance is not completely understood, with several competing models proposed. It is therefore of interest to know if the midgut of *Drosophila*, given its potential in genomics, provides an opportunity for testing these hypotheses.

Despite the wealth of data that has made *Drosophila* an invaluable model system for studying development of structure and function of organ systems, there have been few studies on the structure (Dimitriadis, 1991; Dimitriadis and Kastritsis, 1984; Filshie et al., 1971; Gartner, 1985) and function (Romero et al., 2000; Sciortino et al., 2001) of the gut. The recent resurgence of interest in the structure and function of *Drosophila* midgut has coincidentally occurred on two fronts. Microperfusion of the midgut and stereological analysis of ultrastructure under controlled conditions (Shanbhag and Tripathi, 2005) has enabled description of the transport properties of the epithelium and analysis of the cellular basis of generation of axial H^+ gradients in different segments. The identification of stem cells in adult midgut and hindgut segments (Lin et al., 2008; Micchelli and Perrimon, 2006; Ohlstein and Spradling, 2006; Takashima et al., 2008) has shown that *Drosophila* midgut epithelial development and maintenance is analogous to mammalian intestinal crypt development. In this review, we focus on the structural specialization of the epithelium of various regions of the midgut and the mechanisms of acid–base transport by this epithelium in larval and adult stages.

Structure of midgut regions

Insight into the structural organization and regional specialization of the *Drosophila* midgut was first obtained by Filshie et al. (Filshie et al., 1971). Gartner (Gartner, 1985) attempted the first

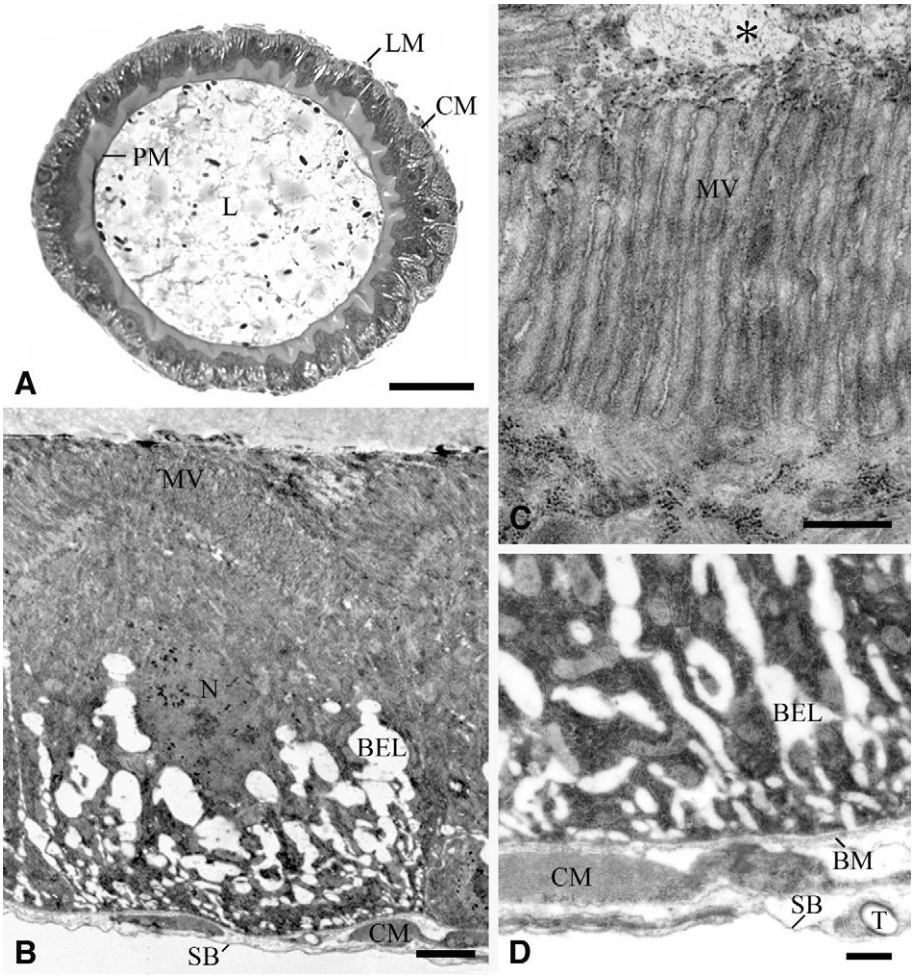

Fig. 7. Unperfused adult posterior midgut. (A) Single layer of cuboidal cells, inner circular muscle (CM) and outer longitudinal muscle (LM); magnification ×680; scale bar, 25 μm. (B) The basal region of the cell shows highly dilated basal extracellular labyrinth (BEL); magnification ×5700; scale bar, 2.0 μm. (C) Densely packed microvilli (MV); asterisk, ectoperitrophic space; magnification ×28,500; scale bar, 0.5 μm. (D) Basal aspect of an adult posterior midgut epithelial cell with highly dilated BEL. BM, basement membrane; CM, circular muscle; SB, serosal barrier; T, tracheole; magnification ×15,000; scale bar, 0.5 μm.

stereological analysis of the anterior part of the adult epithelium and observed the presence of regenerative cells and the primary epithelial cells of the anterior midgut only, concluding that these were the only two cell types lining the epithelium. Dimitriadis and Kastritsis (Dimitriadis and Kastritsis, 1984; Dimitriadis, 1991), however, analysed the entire midgut in detail and identified at least three specialized regions of the midgut and made the first attempts to correlate the structure of the individual segments and cell types with function. The identification of the middle segment as an acid-secreting part has been verified and has invited immediate comparison with mammalian epithelia, particularly the gastric epithelium containing parietal cells (Baumann, 2001; Dubreuil, 2004; Dubreuil et al., 1998; Dubreuil et al., 2001; Yao and Forte, 2003).

Larval midgut

For any epithelium, a controlled study requires access to both sides of the epithelium, and for a tubular epithelium requires perfusion of the lumen. This has been achieved for the larval *Drosophila* midgut (Shanbhag and Tripathi, 2005), allowing stereological analysis of epithelial geometry simultaneously with physiological studies. Fig. 1 shows the basic organization of the midgut into at least three separate parts: an anterior near-neutral part, a strongly acidic middle segment and a third zone of increasing alkalinity. The posterior midgut epithelium has been best studied, but in principle all segments are amenable to perfusion studies. The epithelium is tight because of long septa between cells (Fig. 2A). Notable among its properties is the amplification of the apical and basal membranes (Fig. 3A,B,C, Table 1). The value of ultrastructure is further shown in its sensitivity in detecting changes produced by physiological manoeuvres such as Na^+ replacement, which can produce massive and irreversible loss of plasma membrane (Fig. 3D–I), particularly when done on the basal side. The apical and basal membranes have portasome-like particles (Fig. 2D,E, inset) indicative of H^+ V-ATPase location on both membranes.

Adult midgut

The adult midgut is segmented into anterior, middle and posterior regions (Fig. 4). The basic membrane areas and volumes of the anterior and posterior midgut of the adult epithelium (Table 2) reveal that their transport role is modest and correlate with smaller pH gradients. The anterior segment is probably absorptive and

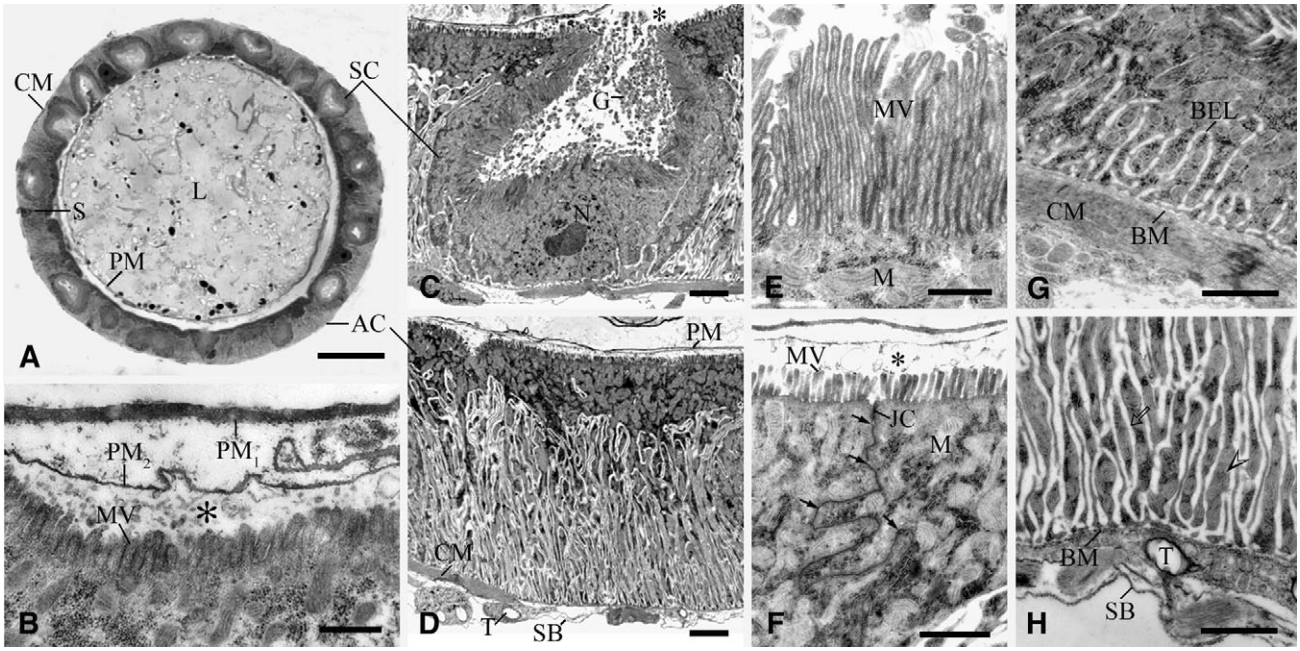

Fig. 8. Unperfused adult middle (or acidic) midgut. (A) Epithelial layer with alternating absorptive cells (AC) and cup-shaped secretory cells (SC). This region also contains several regenerative or stem cells (S). CM, circular muscle; L, lumen; PM, peritrophic membrane; magnification ×560; scale bar, 25 μm. (B) Section through an apical region of an absorptive cell enclosed by double-layered peritrophic membranes PM_1 and PM_2 enclosing the ectoperitrophic space (asterisk) between the microvillar brush-border (MV) and PM_2; magnification ×27,000; scale bar, 0.5 μm. (C) Section through a cup-shaped secretory cell with basally located nucleus (N). Apical region of the cell has a well-developed brush-border (see E) and the basal region shows few membrane infoldings (see G). The cavity is usually filled with vesicles and secretory granules (G), and opens into the ectoperitrophic space (asterisk); magnification ×4100; scale bar, 2.0 μm. (D) Section through an absorptive cell depicting the extensive array of deep parallel basal extracellular labyrinth extending to two-thirds of the cell height and perpendicular to the basement membrane (see H). CM, circular muscle; SB, serosal barrier; T, tracheole; magnification ×3900; scale bar, 2.0 μm. (E) Apical region of a secretory cell contains long and densely packed MV. Several large mitochondria (M) are present in the cytoplasm but not in the microvilli; magnification ×26,400; scale bar, 0.5 μm. (F) Section through an apical region of two adjacent absorptive cells showing small loosely packed MV. These cells also contain many large M. The long intracellular junctional complex (JC) has several dilations (arrows) but no lateral intracellular spaces; magnification ×15,000; scale bar, 1.0 μm. (G) Section through the basal region of a secretory cell shows very few evaginations of basal extracellular labyrinth (BEL). BM, basement membrane; CM, circular muscle; magnification ×16,000; scale bar, 1.0 μm. (H) Magnified view of the basal region of the absorptive cell (cf. D) with extensive array of BEL (open arrow) enclosed by BM. Several mitochondria (open arrowhead) lie parallel with their membranes closely opposed to the plasma membrane of the basal infoldings. The thin serosal barrier (SB) isolates the compartment between the BM and the haemolymph. T, tracheole. Magnification ×16,700; scale bar, 1.0 μm.

Table 3. Quantitative ultrastructural analysis of bilaterally perfused middle midgut segment in adult *Drosophila melanogaster*

	Unperfused middle (acidic) segment		Perfused middle (acidic) segment	
	Secretory cell	Absorptive cell	Secretory cell	Absorptive cell
Apical membrane gain by folding (per cell)	2.35	1.24	2.48	1.45
Mean microvillar amplification*	93.7±2.8 (*N*=9)	8.9±0.8 (*N*=9)	70.3±3.4 (*N*=8)	4.1±0.4 (*N*=6)
Mean luminal membrane surface (excluding microvilli) (10^3 μm^2 mm^{-1} length)	459.6	242.9	565.1	397.7
Mean apical membrane area (10^6 μm^2 mm^{-1} length)	43.0	2.2	39.7	1.6
Mean basement membrane surface area (10^3 μm^2 mm^{-1} length)	195.7	195.7	260.3	285.8
Basal extracellular labyrinth amplification*	10.0±1.2 (*N*=20)	94.3±7.2 (*N*=26)	7.7±0.8 (*N*=6)	153.2±7.8 (*N*=14)
Mean cell volume (10^6 μm^3 mm^{-1} length)	1.62	1.62	1.09	2.48
Mean basal extracellular labyrinth volume (10^6 μm^3 mm^{-1} length)	0.04 (2.3%)	0.56 (34.6%)	0.08 (7.5%)	1.18 (26.3%)
Mean basal membrane area (10^6 μm^2 mm^{-1} length)	2.0	18.4	2.1	43.8
Ratio of microvillar amplification/BEL amplification	9.37	0.09	9.12	0.03

*Data are means ± s.e.m.

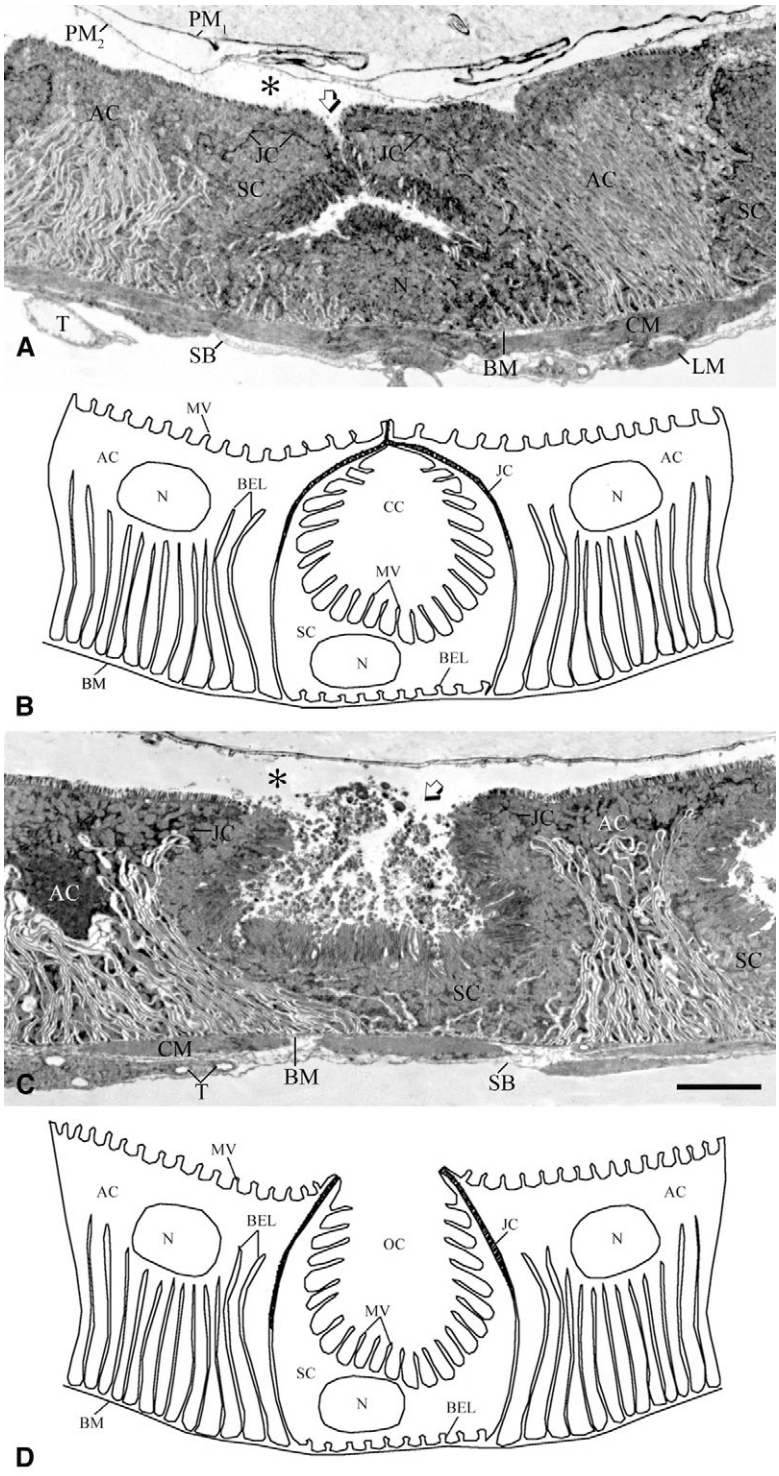

Fig. 9. Unperfused adult middle midgut. (A,C) Low-magnification electron micrographs of a secretory cell (SC) located between two absorptive cells (AC) in closed and open configurations (open arrow). The secretory cell cavity in the open state contains electron-dense granules and vesicles that are liberated into the ectoperitrophic space (asterisk) of the midgut; magnification ×2600; scale bar, 5.0 μm. (B,D) Diagrammatic representations of a secretory cell (SC) located between two absorptive cells (AC) in open and closed configurations (also see Fig. 10A,E). The luminal surface of SC has long, densely populated microvilli (MV), and the basal surface displays few infoldings (BEL). Absorptive cells (AC) have very short and sparsely distributed MV but long and extensive parallel arrays of BEL. BM, basement membrane; CC, closed cavity; CM, circular muscle; JC, intercellular junctional complex; LM, longitudinal muscle; N, nucleus; OC, open cavity; PM_1 and PM_2, peritrophic membranes; SB, serosal barrier; T, tracheole.

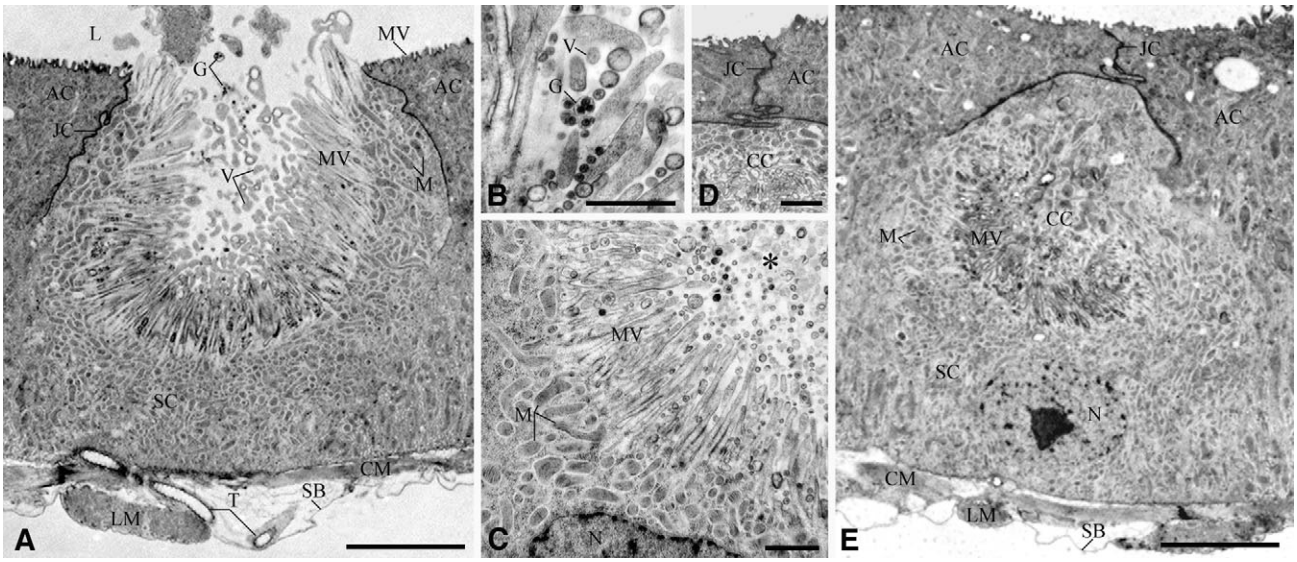

Fig. 10. Perfused adult middle midgut. (A). Section through a secretory cell (SC) with apical cavity open to the lumen (L). The peritrophic membrane is washed off, and intact microvilli (MV) are directly in contact with the luminal solution. The cell contains a large number of secretory granules (G), vesicles (V) and mitochondria (M); CM, circular muscle; LM, longitudinal muscle; SB, serosal barrier; T, tracheole; magnification ×5000; scale bar, 5.0 μm. (B) Magnified view of apical region of a secretory cell shows vesicles with single or many electron-dense granules (G) arising mainly from the base of the adjacent microvilli and many electron-lucent vesicles (V) that bud off usually from the tip of the MV; magnification ×18,700; scale bar, 1.0 μm. (C) Section through a portion of the cavity (asterisk) of the secretory cell, with many secretory granules and vesicles. M, mitochondria; MV, microvilli; N, nucleus; magnification ×11,300; scale bar, 1.0 μm. (D) Intercellular junctional complex (JC) of an absorptive cell(s) seen closing the apical aperture of the secretory cavity; magnification ×9300; scale bar, 1.0 μm. (E). Section through a secretory cell (SC) in the same plane shows the apical cell cavity closed by the intercellular JC of an absorptive cell (AC). CC, closed cavity; CM, circular muscle; LM, longitudinal muscle; M, mitochondria; SB, serosal barrier; magnification ×5000; scale bar, 5.0 μm.

confirms the basic observations of Gartner (Gartner, 1985) pertaining to the anterior midgut only but also reveals that there is a degree of variation of the anterior gut along its length (Fig. 4B,C, Fig. 5, Fig. 6). Posterior segment cells (Fig. 4E, Fig. 7) have an extensively dilated basal extracellular labyrinth, with a volume larger than that of anterior segment cells, indicating more fluid reabsorption in the posterior segment (Tripathi and Boulpaep, 1989). Much less is known of the role of this epithelium in adults, which requires further study in both ultrastructure and physiology.

The middle adult acidic segment (Fig. 4D; Figs 8–10) has attracted a good deal of attention for its striking architecture, with alternate cells 'facing' opposite directions. It would be appropriate to refer to them as secretory and absorptive cells on account of the great asymmetry of their apical and basal membranes (Fig. 8D–H). Cells of the middle segment are alternately absorptive (apically amplified ≈9-fold, basally >90-fold) and secretory (apically amplified by >90-fold and basally ≈10-fold). The terminology suggested is based on the direction of net transport predicted on areal considerations alone. Table 3 shows that the apical and basal membranes of these two cell types are amplified more than 100-fold in either direction; their back-to-back geometry predicts significant recycling of solutes and water and provides a structural basis for bidirectional transport. The function of the secretory cells, composition of the secreted contents, regulation of secretion, and membrane turnover are still not clear, despite many studies (Lehane and Billingsley, 1996; Yao and Forte, 2003). The apical membranes form a cavity that can be seen spontaneously in either 'open' or 'closed' configuration (Figs 9 and 10) discharging membrane-bound granular material.

Bidirectional transport in individual regions

The identification of morphologically distinct segments of the midgut implies that controlled study of each segment is necessary before one can integrate the information for the entire midgut. Larvae, being voracious feeders, have a highly active midgut epithelium, as evidenced by the generation of much steeper pH gradients compared with adults (Shanbhag and Tripathi, 2005; Shanbhag and Tripathi, 2008) (Figs 11, 12). Similar gradients have been seen in a wide variety of insect midgut epithelia (Dadd, 1975; Boudko et al., 2001b; Corena et al., 2002; Dow, 1986; Moffett and Cummings, 1994; Onken et al., 2008; Zhuang et al., 1999). Regardless of the direction of secretion of acid or base, the energetics of transport in insect epithelia is believed to be primarily driven by vacuolar or H^+ V-ATPases in the Malpighian tubule and also the midgut (Beyenbach, 2001; Dow and Davies, 2001). The fluxes of other electrolytes have been proposed to be driven as secondary transport processes. Furthermore, it is also possible that many of the membrane transporters in insects could be isoforms of mammalian transporters that do not bind inhibitors or agonists as they do in mammals. In the posterior larval midgut of *Drosophila*, a variety of inhibitors had no effect on transport that was still sensitive to bafilomycin-A_1 (Shanbhag and Tripathi, 2005).

Larval midgut

The other general feature of acid and base transport in the midgut epithelia of many insects is that there is a carbonic anhydrase (CA)-catalysed pool of H^+ from which the H^+ V-ATPases pump (Corena et al., 2002; Corena et al., 2005; Ridgway and Moffett, 1986; Seron et al., 2004). The location of this pool is a subject of active study as many enzymes are glycosylphosphatidylinositol-anchored and it

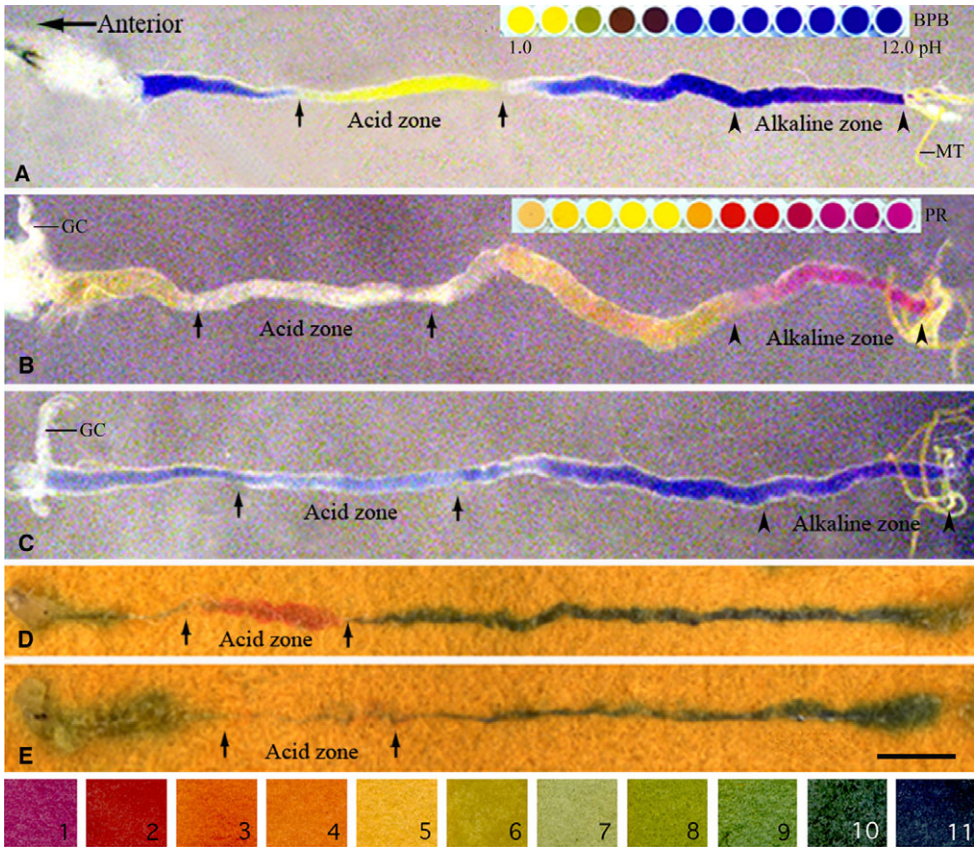

Fig. 11. Midguts of 3rd instar *Drosophila* larvae. (A,B) Larvae fed with food containing dyes alone or together with acetazolamide (C) to detect luminal pH. GC, gastric caeca; MT, Malpighian tubules. (A) Acidification was detected in the middle midgut (acid zone), where Bromophenol Blue (BPB) dye changed from blue to yellow (pH<3.0). (B) Very strong alkalinization was detected in the posterior half of the posterior midgut (alkaline zone), where Phenol Red (PR) dye changed from red to dark pink (pH>10.0). (C) Acetazolamide (100 μmol l^{-1}) in food containing BPB led to dissipation of pH gradients in the larval midgut. (D) Luminal content pH detected by pH paper shows a distinct acid-secreting zone (acid zone, ochre, pH<3) and posterior alkaline zone (dark green). (E) Acetazolamide (100 μmol l^{-1}) in food dissipated the pH gradients in the acid zone. Numbered panels below denote colours generated on universal pH paper by pH standards of 1–11. Scale bar, 1 mm.

is possible to localize these pools to either intracellular or extracellular or both compartments. Strong CA activity was localized at the apical membranes of goblet cells in the anterior and middle midgut region of *Manduca sexta* that is associated with the lumen alkalinization, but no CA activity was found in the posterior midgut goblet cells. Lepidopteran midgut is also divided into regions that show a substantial degree of structural and functional differentiation (Ridgway and Moffett, 1986).

The localization of CA in the *Drosophila* midgut has not yet been achieved, but there are several interesting approaches that can be tried. Corena et al. have localized CA in the mosquito midgut (Corena et al., 2004), and a similar approach with membrane permeant and impermeant inhibitor would be a valuable approach. The removal of the peritrophic membrane by microperfusion improves access of the luminal perfusate to the apical membrane. It is possible that the *in vivo* conditions of the peritrophic space may be altered in terms of enzymes like CA that are located there (Smith et al., 2007), but there is good reason to assume that the intracellular enzyme-catalysed H^+ pool is intact in perfused midguts, as shown below. As the ectoperitrophic space is a likely candidate for such a location, it would be important to verify this localization with antibodies to CA9 in both perfused and unperfused preparations where the peritrophic membrane is intact (Fig. 2C). The dissipation of the acid gradient by inhibition of CA with acetazolamide (Shanbhag and Tripathi, 2008) is easily detected on pH paper (Fig. 11D,E). However, the effects of inhibition of CA involved in base secretion in the posterior midgut are not easily detected by this simple method. One then has to rely on a more sensitive method (e.g. ion-selective microelectrodes) to detect acid or base fluxes. Such an approach is shown in Fig. 13.

In Fig. 13A, which shows measurement of intracellular pH, along with other membrane parameters, in the perfused larval midgut, acetazolamide alkalinizes the cell when applied to the bath; these effects are also seen from the lumen. This is clear evidence that extrusion of acid and base is rate limited in the H^+ pool. There has been some uncertainty about the localization of the ATPase, particularly in view of data on the Malpighian tubule and the mosquito midgut (Beyenbach et al., 2000; O'Donnell et al., 1996; Wieczorek et al., 1999; Wieczorek et al., 2003). One line of evidence for a basal location of the ATPase in the *Drosophila* posterior midgut (Shanbhag and Tripathi, 2005), where the lumen is strongly alkaline, is the presence of portasome-like structures in the BEL (Fig. 2E, inset). The intracellular pH being more alkaline than the BEL or unstirred layer of the bath (Fig. 13A) provides even

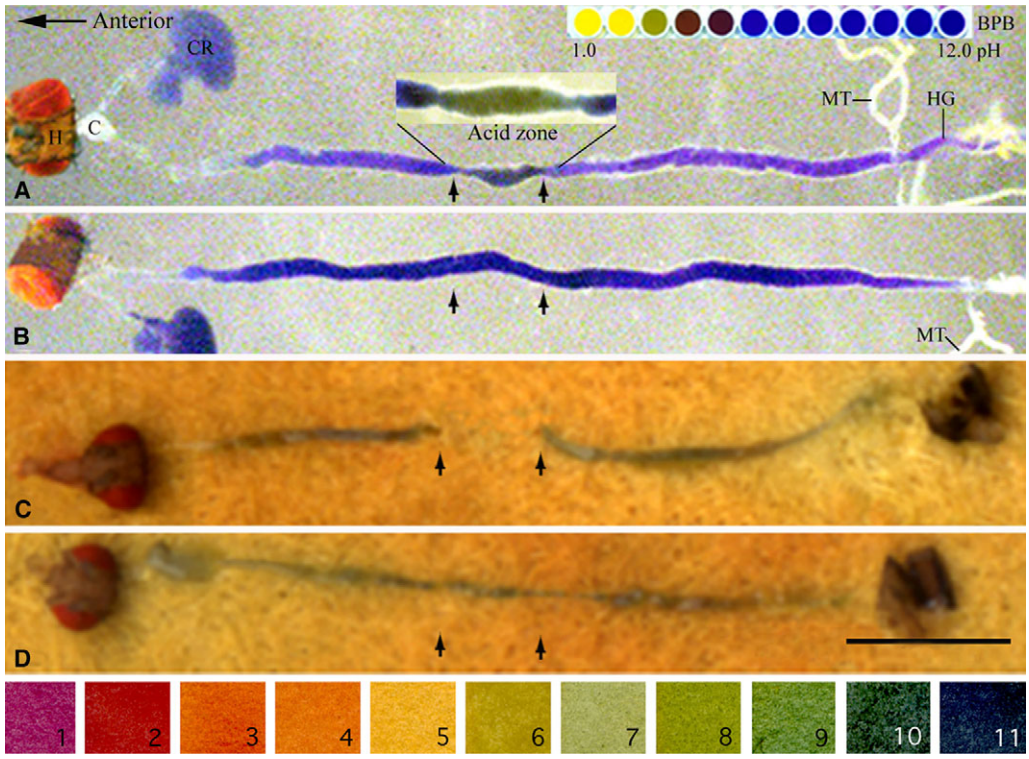

Fig. 12. Carbonic anhydrase in the adult midgut. (A) Acidification was detected in the middle midgut (arrows, acid zone) where the colour of Bromophenol Blue (BPB) dye changed from blue to greenish brown (acid zone, pH<4.0); C, cardia; CR, crop; H, head; HG, hindgut; MT, Malpighian tubules. (B) Acetazolamide (100 μmol l^{-1}) in food dissipated this gradient. (C) Luminal content pH detected by pH paper showed a distinct acid-secreting zone (arrows, pH<5) in the adult middle midgut. (D) Acetazolamide (100 μmol l^{-1}) in food abolishes this acidification (arrows). Numbered panels below denote colours generated on universal pH paper by pH standards of 1–11. Scale bar, 1 mm.

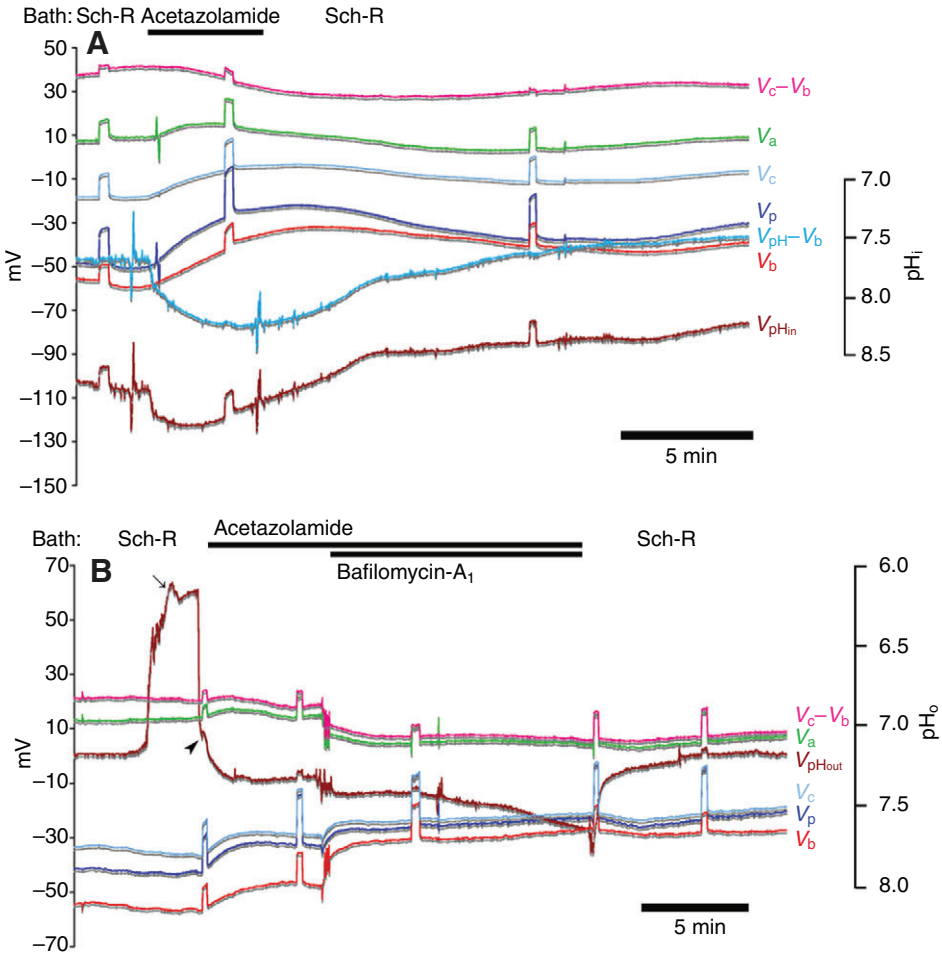

Fig. 13. Carbonic anhydrase and H^+ V-ATPase in the larval posterior midgut. (A) Intracellular pH measured in control solution (Sch-R) containing equal amounts of Schneider insect medium and insect Ringer perfusing the lumen and in the bath. V_a, apical membrane potential; V_b, basal membrane potential; V_c, transepithelial potential at collection end; V_p, transepithelial potential at perfusion end; $V_{pH_{in}}$, potential of ion-selective microelectrode; V_{pH}–V_b, intracellular pH corrected for membrane potential, referenced to ordinate at right. Acetazolamide (100 μmol l^{-1}) applied to the bath reversibly alkalinizes the cell. (B) Extracellular scan of basal unstirred layer pH with an ion-selective microelectrode whose potential $V_{pH_{out}}$ is shown as the brown trace, referenced to the ordinate on the right. In Sch-R, the extracellular pH of the bulk solution of the bath is 7.2. The pH microelectrode was advanced towards the gut wall by a piezo-stepper and positioned close to the serosal barrier and basal extracellular labyrinth (BEL; arrow); the increasingly positive $V_{pH_{out}}$ potential reflects the pH gradient at the basal surface. The pH electrode was then retracted away to about 20 μm from the gut wall (arrowhead). Acetazolamide (100 μmol l^{-1}) applied to the bath alkalinized the extracellular pH. Bafilomycin-A_1 (1.5 μmol l^{-1}) applied to the bath in addition to acetazolamide in the bath further alkalinized the extracellular pH. Washout with control Ringer restored H^+ extrusion by the midgut, as seen by the positive change in $V_{pH_{out}}$ at the end of the trace.

stronger evidence for the predominantly basal location of the H^+ V-ATPase. Thirdly, sensitivity to bafilomycin is also greater in this preparation from the bath side, with hardly any effect detected from the lumen. Thus, one can measure acid extrusion rates from the basal side (Fig. 13B), and see its reversible inhibition by acetazolamide, even without the peritrophic membrane (from the lumen or bath) and bafilomycin (from the bath only).

Adult midgut

Perfusion of each midgut region is important to know the overall driving forces for ions in each segment. Representative traces for three adult segments are shown in Fig. 14 along with basic membrane potential data under free-flow conditions in control Ringer and taking into account the fact that the ends of the segments are damaged but electrically isolating the lumen from the bath. The anterior region has a low transepithelial potential; the middle and posterior segments have a transepithelial potential whose polarity favours net H^+ flux, which can occur passively for the observed gradients. Therefore, primary and secondary active transport processes have to be independently tested in these segments along with a complete characterization of all electrochemical driving forces and passive properties of individual cell membranes and the paracellular pathway. Whereas the larval gut has a predominant H^+ V-ATPase as primary transporter, the situation in the adult is far from clear.

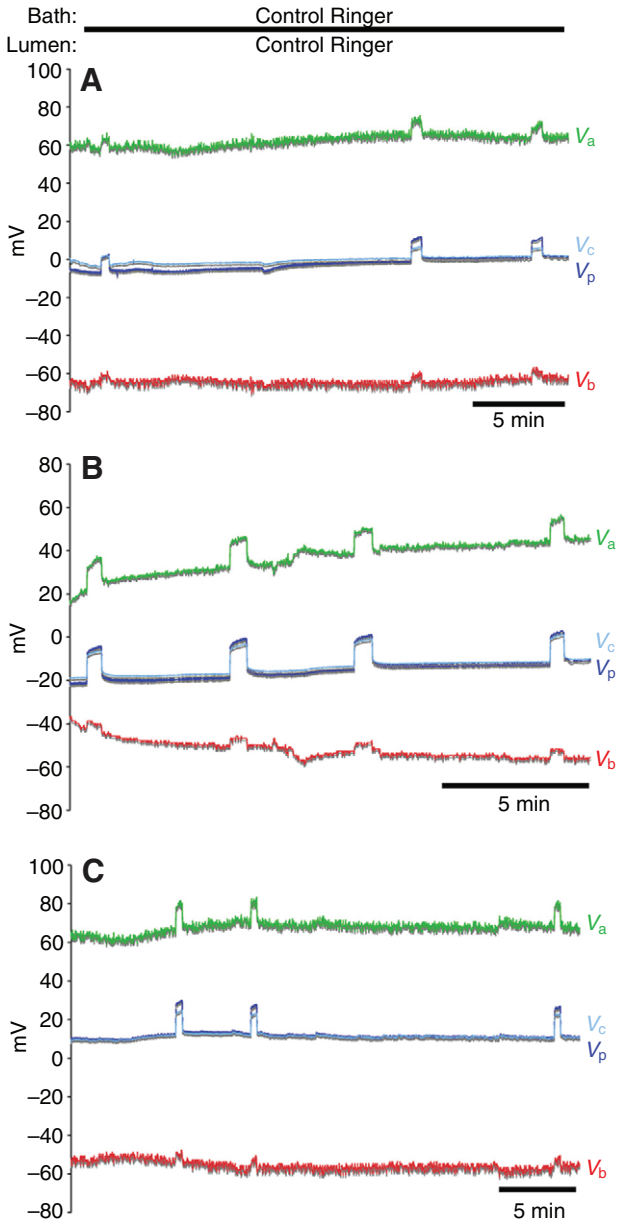

Fig. 14. (A–C) Adult midgut transepithelial potentials recorded from the anterior, middle and posterior segments, respectively, of *Drosophila* by the perfusion (V_p), collection (V_c) micropipettes and the basal cell membrane potential (V_b), after bilateral HCO_3^- Ringer (control Ringer) substitution. Current pulses (≈100 nA) cause displacements of V_a, V_b, V_c and V_p. V_a, apical membrane potential.

Microperfusion and electrophysiological approaches have given us new tools to investigate membrane transport processes in an important genomic organism with many characterized mutations, e.g. *labial* (Dubreuil et al., 1998), where individual cuprophilic cells may be absent. For a complete understanding of the role of pH gradients in the *Drosophila* gut, experiments need to be designed to supplement the approach shown here with newer techniques. For instance, it is still not clear how base is secreted across the apical membranes in the posterior midgut in either larva or adult. It would be of interest to examine whether transporters like NDAE1 (Romero et al., 2000; Sciortino et al., 2001) are involved in the exit of base in the posterior midgut. Likewise, the transport of other electrolytes and osmolytes needs clarification, as it is very likely to be linked to the transport of acid and base in this epithelium. The approach shown here can contribute to this end.

We thank our colleagues T. V. Abraham and J. N. Parmar for their unfailing support and Professor L. C. Padhy for valuable discussions. Supported by Interdisciplinary Programme 11-R&D-TFR-5.02-1106.

References

Anderson, E. and Harvey, W. R. (1966). Active transport by the *Cecropia* midgut. II. Fine structure of the midgut epithelium. *J. Cell Biol.* **31**, 107-134.
Baumann, O. (2001). Posterior midgut epithelial cells differ in their organization of the membrane skeleton from other *Drosophila* epithelia. *Exp. Cell Res.* **270**, 176-187.
Beyenbach, K. W. (2001). Energizing epithelial transport with the vacuolar H^+-ATPase. *News Physiol. Sci.* **16**, 145-151.
Beyenbach, K. W., Pannabecker, T. L. and Nagel, W. (2000). Central role of the apical membrane H^+-ATPase in electrogenesis and epithelial transport in Malpighian tubules. *J. Exp. Biol.* **203**, 1459-1468.
Boudko, D. Y., Moroz, L. L., Linser, P. J., Trimarchi, J. R., Smith, P. J. S. and Harvey, W. R. (2001a). *In situ* analysis of pH gradients in mosquito larvae using non-invasive, self-referencing, pH-sensitive microelectrodes. *J. Exp. Biol.* **204**, 691-699.
Boudko, D. Y., Moroz, L. L., Harvey, W. R. and Linser, P. J. (2001b). Alkalinization by chloride/bicarbonate pathway in larval mosquito midgut. *Proc. Natl. Acad. Sci. USA* **98**, 15354-15359.
Cioffi, M. (1979). The morphology and fine structure of the larval midgut of a moth (*Manduca sexta*) in relation to active ion transport. *Tissue Cell* **11**, 467-479.
Clements, A. N. (1992). *The Biology of Mosquitoes*. London: Chapman and Hall.
Corena, M. P., Seron, T. J., Lehman, H. K., Ochrietor, J. D., Kohn, A., Tu, C. and Linser, P. J. (2002). Carbonic anhydrase in the midgut of larval *Aedes aegypti*: cloning, localization and inhibition. *J. Exp. Biol.* **205**, 591-602.
Corena, M. P., Fiedler, M. M., VanEkeris, L., Tu, C., Silverman, D. N. and Linser, P. J. (2004). Alkalization of larval mosquito midgut and the role of carbonic anhydrase in different species of mosquitoes. *Comp. Biochem. Physiol.* **137C**, 207-225.
Corena, M. P., VanEkeris, L., Salazar, M. I., Bowers, D., Fiedler, M. M., Silverman, D., Tu, C. and Linser, P. J. (2005). Carbonic anhydrase in the adult mosquito midgut. *J. Exp. Biol.* **208**, 3263-3273.
Dadd, R. H. (1975). Alkalinity within the midgut of mosquito larvae with alkaline-active digestive enzymes. *J. Insect Physiol.* **21**, 1847-1853.
Dimitriadis, V. K. (1991). Fine structure of the midgut of adult *Drosophila auraria* and its relationship to the sites of acidophilic secretion. *J. Insect Physiol.* **37**, 167-177.
Dimitriadis, V. K. and Kastritsis, C. D. (1984). Ultrastructural analysis of the midgut of *Drosophila auraria* larvae: morphological observations and their physiological implications. *Can. J. Zool.* **62**, 659-669.
Dow, J. A. T. (1984). Extremely high pH in biological systems: a model for carbonate transport. *Am. J. Physiol.* **246,** R633-R636.
Dow, J. A. T. (1986). Insect midgut function. *Adv. Insect Physiol.* **19**, 187-328.
Dow, J. A. T. and Peacock, J. M. (1989). Microelectrode evidence for the electrical isolation of goblet cell cavities in *Manduca sexta* middle midgut. *J. Exp. Biol.* **143**, 101-114.

Dow, J. A. T. and Davies, S. A. (2001). The *Drosophila melanogaster* Malpighian tubules. *Adv. Insect Physiol.* **28**, 1-83.
Dow, J. A. T., Davies, S. A., Guo, Y., Graham, S., Finbow, M. E. and Kaiser, K. (1997). Molecular genetic analysis of V-ATPase function in *Drosophila melanogaster*. *J. Exp. Biol.* **200**, 237-245.
Dubreuil, R. R. (2004). Copper cells and stomach acid secretion in the *Drosophila* midgut. *Int. J. Biochem. Cell Biol.* **36**, 745-752.
Dubreuil, R. R., Frankel, J., Wang, P., Howrylak, J., Kappil, M. and Grushko, T. A. (1998). Mutations of α spectrin and *labial* block cuprophilic cell differentiation and acid secretion in the middle midgut of *Drosophila* larvae. *Dev. Biol.* **194**, 1-11.
Dubreuil, R. R., Grushko, T. and Baumann, O. (2001). Differential effects of a *labial* mutation on the development, structure, and function of stomach acid-secreting cells in *Drosophila melanogaster* larvae and adults. *Cell Tissue Res.* **306**, 167-178.
Filshie, B. K., Poulson, D. F. and Waterhouse, D. F. (1971). Ultrastructure of the copper-accumulating region of the *Drosophila* larval midgut. *Tissue Cell* **3**, 77-102.
Gartner, L. P. (1985). The fine structural morphology of the midgut of adult *Drosophila*: a morphometric analysis. *Tissue Cell* **17**, 883-888.
Lehane, M. J. and Billingsley, P. F. (1996). *Biology of the Insect Midgut*. London: Chapman and Hall.
Lin, G., Xu, N. and Xi, R. (2008). Paracrine Wingless signalling controls self-renewal of *Drosophila* intestinal stem cells. *Nature* **455**, 1119-1122.
Maddrell, S. H. P. and O'Donnell, M. J. (1992). Insect Malpighian tubules: V-ATPase action in ion and fluid transport. *J. Exp. Biol.* **172**, 417-429.
Micchelli, C. A. and Perrimon, N. (2006). Evidence that stem cells reside in the adult *Drosophila* midgut epithelium. *Nature* **439**, 475-479.
Moffett, D. F. and Cummings, S. A. (1994). Transepithelial potential and alkalization in an *in situ* preparation of tobacco hornworm (*Manduca sexta*) midgut. *J. Exp. Biol.* **194**, 341-345.
O'Donnell, M. J. and Spring, J. H. (2000). Modes of control of insect Malpighian tubules: synergism, antagonism, cooperation and autonomous regulation. *J. Insect Physiol.* **46**, 107-117.
O'Donnell, M. J., Dow, J. A. T., Huesmann, G. R., Tublitz, N. J. and Maddrell, S. H. P. (1996). Separate control of anion and cation transport in Malpighian tubules of *Drosophila melanogaster*. *J. Exp. Biol.* **199**, 1163-1175.
Ohlstein, B. and Spradling, A. (2006). The adult *Drosophila* posterior midgut is maintained by pluripotent stem cells. *Nature* **439**, 470-474.
Okech, B. A., Boudko, D. Y., Linser, P. J. and Harvey, W. R. (2008). Cationic pathway of pH regulation in larvae of *Anopheles gambiae*. *J. Exp. Biol.* **211**, 957-968.
Onken, H., Moffett, S. B. and Moffett, D. F. (2006). The isolated anterior stomach of larval mosquitoes (*Aedes aegypti*): voltage-clamp measurements with a tubular epithelium. *Comp. Biochem. Physiol.* **143A**, 24-34.
Onken, H., Moffett, S. B. and Moffett, D. F. (2008). Alkalinization in the isolated and perfused anterior midgut of the larval mosquito, *Aedes aegypti*. *J. Insect Sci.* **8**, 1-20.
Patrick, M. L., Aimanova, K., Sanders, H. R. and Gill, S. S. (2006). P-type Na^+/K^+-ATPase and V-type H^+-ATPase expression patterns in the osmoregulatory organs of larval and adult mosquito *Aedes aegypti*. *J. Exp. Biol.* **209**, 4638-4651.
Ridgway, R. L. and Moffett, D. F. (1986). Regional differences in the histochemical localization of carbonic anhydrase in the midgut of tobacco hornworm (*Manduca sexta*). *J. Exp. Zool.* **237**, 407-412.
Romero, M. F., Henry, D., Nelson, S., Harte, P. J., Dillon, A. K. and Sciortino, C. M. (2000). Cloning and characterization of a Na^+-driven anion exchanger (NDAE1). *J. Biol. Chem.* **275**, 24552-24559.
Sciortino, C. M., Shrode, L. D., Fletcher, B. R., Harte, P. J. and Romero, M. F. (2001). Localization of endogenous and recombinant Na^+-driven anion exchanger protein NDAE1 from *Drosophila melanogaster*. *Am. J. Physiol.* **281**, C449-C463.
Seron, T. J., Hill, J. and Linser, P. J. (2004). A GPI-Linked carbonic anhydrase expressed in the larval mosquito midgut. *J. Exp. Biol.* **207**, 4559-4572.
Shanbhag, S. and Tripathi, S. (2005). Electrogenic H^+ transport and pH gradients generated by a V-H^+-ATPase in the isolated perfused larval *Drosophila* midgut. *J. Membrane Biol.* **206**, 61-72.
Shanbhag, S. and Tripathi, S. (2008). Segmental bidirectional transport of H^+ in the adult *Drosophila* midgut. *Comp. Biochem. Physiol.* **150A**, A11.29, S138.
Smith, K. E., VanEkeris, L. A. and Linser, P. J. (2007). Cloning and characterization of AgCA9, a novel α-carbonic anhydrase from *Anopheles gambiae* Giles *sensu stricto* (Diptera: Culicidae) larvae. *J. Exp. Biol.* **210**, 3919-3930.
Smith, K. E., VanEkeris, L. A., Okech, B. A., Harvey, W. R. and Linser, P. J. (2008). Larval anopheline mosquito recta exhibit a dramatic change in localization patterns of ion transport proteins in response to shifting salinity: a comparison between anopheline and culine larvae. *J. Exp. Biol.* **211**, 3067-3076.
Takashima, S., Mkrtchyan, M., Hartenstein, A. Y., Merriam, J. R. and Hartenstein, V. (2008). The behaviour of *Drosophila* adult hindgut stem cells is controlled by Wnt and Hh signalling. *Nature* **454**, 651-655.
Tripathi, S. and Boulpaep, E. L. (1989). Mechanisms of water transport by epithelial cells. *Q. J. Exp. Physiol.* **74**, 385-417.
Volkmann, A. and Peters, W. (1989a). Investigations on the midgut caeca of mosquito larvae. I. Fine-structure. *Tissue Cell* **21**, 243-251.
Volkmann, A. and Peters, W. (1989b). Investigations on the midgut caeca of mosquito larvae. II. Functional-aspects. *Tissue Cell* **21**, 253-261.
Wieczorek, H., Brown, D., Grinstein, S., Ehrenfeld, J. and Harvey, W. R. (1999). Animal plasma membrane energization by proton-motive V-ATPases. *BioEssays* **21**, 637-648.
Wieczorek, H., Huss, M., Merzendorfer, H., Reineke, S., Vitavska, O. and Zeiske, W. (2003). The insect plasma membrane H^+ V-ATPase: intra-, inter-, and supramolecular aspects. *J. Bioenerg. Biomembr.* **35**, 359-366.
Yao, X. and Forte, J. G. (2003). Cell biology of acid secretion by the parietal cell. *Annu. Rev. Physiol.* **65**, 103-131.
Zhuang, Z., Linser, P. J. and Harvey, W. R. (1999). Antibody to H^+ V-ATPase subunit E colocalizes with portasomes in alkaline larval midgut of freshwater mosquito (*Aedes aegypti*). *J. Exp. Biol.* **202**, 2449-2460.